Received: 17 July 2023 | Revised: 22 December 2023 | Accepted: 22 January 2024

DOI: 10.1002/nbm.5122

RESEARCH ARTICLE

NMR IN BIOMEDICINE WILEY

Amide proton transfer weighted imaging in pediatric neuro-oncology: initial experience

Iris V. Obdeijn[1] | Evita C. Wiegers[1] | Lejla Alic[2] | Sabine L. A. Plasschaert[3] | Mariëtte E. G. Kranendonk[4] | Hans M. Hoogduin[1] | Dennis W. J. Klomp[1] | Jannie P. Wijnen[1] | Maarten H. Lequin[3,5]

[1]Center for Image Sciences, High Field MR Research Group, University Medical Center Utrecht, Utrecht, The Netherlands

[2]Magnetic Detection and Imaging Group, Technical Medical Center, University of Twente, Enschede, The Netherlands

[3]Department of Pediatric Neuro-Oncology, Princess Máxima Center for Pediatric Oncology, Utrecht, The Netherlands

[4]Department of Diagnostic Laboratory, Princess Máxima Center for Pediatric Oncology, Utrecht, The Netherlands

[5]Department of Radiology and Nuclear Medicine, University of Medical Center Utrecht, Utrecht, The Netherlands

Correspondence
Jannie P. Wijnen, Center for Image Sciences, Department of High Field MR Research Group, University Medical Center Utrecht, Heidelberglaan 100, 3584 CX Utrecht, The Netherlands.
Email: jwijnen@umcutrecht.nl

Funding information
Wilhelmina Kinderziekenhuis; Nederlandse Organisatie voor Wetenschappelijk Onderzoek

Abstract

Amide proton transfer weighted (APTw) imaging enables in vivo assessment of tissue-bound mobile proteins and peptides through the detection of chemical exchange saturation transfer. Promising applications of APTw imaging have been shown in adult brain tumors. As pediatric brain tumors differ from their adult counterparts, we investigate the radiological appearance of pediatric brain tumors on APTw imaging. APTw imaging was conducted at 3 T. APTw maps were calculated using magnetization transfer ratio asymmetry at 3.5 ppm. First, the repeatability of APTw imaging was assessed in a phantom and in five healthy volunteers by calculating the within-subject coefficient of variation (wCV). APTw images of pediatric brain tumor patients were analyzed retrospectively. APTw levels were compared between solid tumor tissue and normal-appearing white matter (NAWM) and between pediatric high-grade glioma (pHGG) and pediatric low-grade glioma (pLGG) using *t*-tests. APTw maps were repeatable in supratentorial and infratentorial brain regions (wCV ranged from 11% to 39%), except those from the pontine region (wCV between 39% and 50%). APTw images of 23 children with brain tumor were analyzed (mean age 12 years ± 5, 12 male). Significantly higher APTw values are present in tumor compared with NAWM for both pHGG and pLGG ($p < 0.05$). APTw values were higher in pLGG subtype pilocytic astrocytoma compared with other pLGG subtypes ($p < 0.05$). Non-invasive characterization of pediatric brain tumor biology with APTw imaging could aid the radiologist in clinical decision-making.

KEYWORDS
amide proton transfer weighted imaging, pediatric brain tumors, MRI, glioma

Abbreviations: APTw, amide proton transfer weighted; CEST, chemical exchange saturation transfer; FLAIR, fluid-attenuation inversion recovery; FOV, field of view; GM, gray matter; HGG, high-grade glioma; LGG, low-grade glioma; MTR_{asym}, magnetic transfer ratio asymmetry; NAWM, normal-appearing white matter; pHGG, pediatric high-grade glioma; pLGG, pediatric low-grade glioma; ROI, region of interest; T1w-gd, contrast-enhanced T_1-weighted imaging; TSE, turbo spin echo; wCV, within-subject coefficient of variation; WM, white matter; WMc-ROI, WM-ROI of the cerebellum.

1 | INTRODUCTION

Pediatric brain tumors comprise a large heterogeneous group, with the standard diagnostic tool being MRI and histopathology, including molecular diagnostics.[1] Various factors such as tumor pathology, location, metastases, size, and age at the time of diagnosis lead to a wide prognostic range.[2] Low-grade gliomas (LGGs) are the most common type of pediatric brain tumor, with a 10-year overall survival rate of about 90%.[3,4] In contrast, diffuse midline glioma are rare but have a low survival rate (~8–11 months).[5]

Pediatric brain tumors are usually monitored with conventional MRI: that is, T_2-weighted, fluid-attenuation inversion recovery (FLAIR), and contrast-enhanced T_1-weighted imaging (T1w-gd). International guidelines regarding, for example, tumor size and contrast enhancement have been developed to uniformly assess treatment response based on MRI.[6] However, distinction between tumor growth and/or treatment effects can still be challenging using these guidelines.[7,8] Nonetheless, this distinction is crucial to offer the patient the right treatment at the right moment. Insight into tumor biology in vivo may aid in the assessment of brain tumors in clinical decision-making concerning diagnosis and treatment evaluation.

Amide proton transfer weighted (APTw) imaging potentially contributes to non-invasive characterization of pediatric brain tumors. This MR technique, based upon chemical exchange saturation transfer (CEST), exploits the exchange of protons between water and tissue-bound mobile protein and peptide levels.[9] The magnetization of the proton pool of mobile proteins and peptides is selectively saturated through RF irradiation with a frequency-selective RF pulse at 3.5 ppm for APT.[10] Subsequently, the proton pool in the saturated state is transferred to protons in the unsaturated bulk water pool via exchange, causing attenuation of the water signal.[9,10] Quantifying the attenuation of the water signal results in an APTw map indirectly reflecting mobile protein content: that is, high APTw values reflect high tissue levels of mobile proteins.[11]

In adult brain tumors, APTw values correlate with Ki-67, a histopathological cell proliferation marker.[12] Promising applications of APTw imaging in neuro-oncology include differentiation between LGG and high-grade glioma (HGG) and between true tumor progression and pseudoprogression.[11,13,14] Furthermore, APTw imaging is reported as a potential imaging biomarker to assess treatment effects in adult brain tumors.[15,16] However, adult brain tumors differ from pediatric brain tumors in terms of clinical, biological, and radiological appearance.[17,18] Current application of APTw imaging may therefore not be directly translatable to the pediatric population, and careful evaluation is needed to identify its applicability in this population.

This study investigates the radiological appearance of pediatric brain tumors on APTw imaging. Since many pediatric brain tumors contain cysts, which have elevated protein concentration, we also analyzed the effect of suppressing cystic fluids on APTw imaging. In order to understand if APTw imaging can aid in longitudinal assessment of brain tumors, we first investigated its repeatability.

2 | METHODS

The institutional ethical review board (NedMec NL53099.041.15) approved the repeatability study in five healthy volunteers, and written informed consent was obtained before participation in the study. Patient data were evaluated retrospectively, for which ethical approval was waived by the institutional ethical review board.

2.1 | Data acquisition

MR images were acquired from a phantom, five healthy volunteers (adults) and children with a glial brain tumor at a 3 T MR system (Ingenia Elition X, Philips Healthcare, Best, The Netherlands) with a 32-channel receive head coil.

APTw images were acquired with a 3D turbo spin echo (TSE) sequence including seven frequency offsets: that is, $\Delta\omega = -2.7$ ppm, 2.7 ppm, −3.5 ppm, 3.5 ppm (repeated three times with an echo shift, ΔT_E), −4.3 ppm, 4.3 ppm, −1540 ppm (3D APT product option of Philips Healthcare, Best, The Netherlands[19]). The acquisition at 3.5 ppm was repeated three times with a ΔT_E [−0.4, 0, +0.4 ms] to create a three-point TSE–Dixon B_0 map.[20] Imaging parameters were the following: repetition time (T_R), 5925 ms; echo time (T_E), 8.3 ms; echo train length, 174 ms; field of view (FOV), 230 mm × 180 mm × 60 mm; acquired voxel size, 1.8 mm × 1.8 mm × 6.0 mm; number of slices, 10; flip angle, 90°; SENSE, 1.6. The RF pulse amplitude ($B_{1,rms}^{+}$) was set to 2.0 μT and the saturation time was 2 s (pulse train: 40 sinc-Gauss shaped elements of 50 ms, with no interpulse delay (duty cycle 100%)). The recovery time after the last readout and before the saturation phase was 2472 ms. Total scan time was 3 min 45 s.

In healthy volunteers T1w images were acquired (T_R/T_E, 8.1/3.7 ms; FOV, 230 mm × 180 mm × 230 mm, voxel size: 1 mm × 1 mm × 1 mm). In patients FLAIR (T_R/T_E, 4800/318 ms; FOV, 230 mm × 180 mm × 230 mm; voxel size, 1.12 mm × 1.12 mm × 1.12 mm), and T1w-gd (T_R/T_E, 8.1/3.7 ms; FOV, 230 mm × 180 mm × 230 mm, voxel size, 1 mm × 1 mm × 1 mm) imaging were acquired as part of the clinical protocol. APTw images were acquired before gadolinium administration.

2.2 | Processing of APTw maps

Z-spectra were voxel-wise corrected for B_0 inhomogeneity, by applying a frequency shift measured using the TSE–Dixon B_0-map. *Z*-spectra were resampled accordingly. APTw maps were calculated with magnetic transfer ratio asymmetry (MTR_{asym}) (Equation 1).

In a subset of patients, APTw maps were also calculated by MTR_{asym} incorporating fluid suppression (Equation 2), as presented by Keupp and Togao[21] and implemented in the 3D APT product option of Philips Healthcare.

$$MTR_{asym} = \frac{S_{sat}[-3.5] - S_{sat}[+3.5]}{S_0} \tag{1}$$

$$\text{Fluid suppressed } MTR_{asym} = MTR_{asym}\left(2 - \frac{S_{sat}[+3.5] + S_{sat}[-3.5]}{S_0}\right) \tag{2}$$

where S_{sat} and S_0 are signals at frequency offsets of ±3.5 and −1540 ppm, respectively. Processing was performed directly on the scanner (software from Philips, Best, The Netherlands).

2.3 | Repeatability

The repeatability of APTw maps was assessed using a cylindrical phantom filled with 0.9% saline solution and five submerged Falcon tubes. The tubes contained solutions of nicotinamide (20, 50, and 100 mM), glutamate (10 mM), and glycine (20 mM) at pH about 7.0 (range 6.8–7.2—measured with pH indicator strips). Additionally, the repeatability was assessed in five healthy volunteers (mean age, 26 ± 2 years, 3 (60%) females) at an interval of approximately 1 week. In healthy volunteers, APTw scans of two individual brain slabs (i.e., supratentorial brain region and infratentorial brain region) were obtained within one session.

The repeatability was quantified by calculating the within-subject coefficient of variation (wCV) in several regions of interest (ROIs). For the phantom circular ROIs were manually delineated. In healthy volunteers, ROIs of gray matter (GM) and white matter (WM) were segmented (three ROIs in supratentorial brain region; five ROIs in infratentorial brain region—cerebellum ($n = 3$) and pons ($n = 2$)) by a registration-based approach. The ROIs of WM included full segments of brain lobes and also small WM segments, referred to as eroded WM-ROIs. Data S1 gives details about the ROIs in healthy volunteers.

2.4 | Pediatric brain tumors: clinical applicability

Between March 2021 and June 2022 APTw imaging was adopted as part of our clinical protocol and was acquired in 52 children at the neuro-oncology ward of the Princess Maxima Center for Pediatric Oncology in Utrecht, the Netherlands. In this retrospective study, we included pediatric patients with a pathological or radiological confirmed glioma. This concerned children with a suspected viable brain tumor at various clinical time points (e.g., at diagnosis or during treatment follow-up). Patients without tumor residual or a tumor without glial origin were excluded. Data with severe motion artifacts were excluded.

Patients were grouped based on histopathological tumor type, that is, pediatric HGG (pHGG) or pediatric LGG (pLGG). Radiological diagnosis was used in cases in which no histopathology report was available ($n = 5$). Based on histopathology pLGGs were subdivided into pilocytic astrocytoma, other, and unknown (no histopathology available).

APTw values were assessed in each patient in two ROIs:

1. solid tumor, excluding cysts and necrotic tumor areas
2. predefined volume (0.2 mL) of normal-appearing white matter (NAWM) in the temporal lobe or parietal lobe.

The location of the NAWM ROI depended on the brain coverage of the APTw image. If possible, the NAWM ROI was placed in the temporal lobe contralateral to the tumor location; otherwise, the NAWM ROI was placed in the parietal lobe contralateral to the tumor location. FLAIR and T1w-gd images were registered rigidly to the S_0 image of the APTw image using ElastiX.[22] The tumor ROI was manually annotated on the registered FLAIR image in the axial direction using ITK-SNAP 3.6.0.[23] T1w-gd images were used as a reference during annotation. A researcher with 2 years of experience in neuroradiology (I.V.O.) annotated all ROIs in consensus with an experienced pediatric neuro-radiologist (M.H.L.) with 25 years of experience.

2.4.1 | Statistical analysis

Normality for all data was tested using a Shapiro–Wilk test prior to *t*-tests. A paired *t*-test was performed to compare the mean APTw values of tumor and NAWM. Differences in mean APTw values between different histopathological tumor types (pHGG, pLGG, and subtypes of pLGG) were assessed with Student's *t*-tests. The effect of fluid suppression on mean APTw values of solid tumor tissue was analyzed by comparing the mean APTw value with and without fluid suppression using a paired *t*-test. The effects of sex, age, type of therapy, and tumor volume on APTw values of NAWM were analyzed with analysis of covariance to identify confounders. Only age was identified as a confounder and was corrected for in the analysis by using age as a covariate.

Statistical analyses were performed in IBM Statistical Package for the Social Sciences (SPPS) (Version 26, IBM, Armonk, NY, USA).

3 | RESULTS

3.1 | Repeatability

For both experiments (phantom and healthy volunteers), the APTw maps show a strong visual similarity between the two time points (Figure 1 and Data S2), supported by the wCV (Table 1), ranging from 11% to 39% for supratentorial and infratentorial (cerebellar) brain regions, indicating repeatable APTw maps.

In healthy volunteers, the best repeatability was obtained for the GM-ROI of the cerebellum and WM-ROI of the cerebellum (WMc-ROI) (details of ROIs in Data S1). In eroded WM-ROIs (~1.2 mL) the wCV increased by 50% with respect to WM-ROIs. Furthermore, in regions with air–tissue transitions, such as the pontine region, B_0 inhomogeneities affect APTw maps with the consequence that the repeatability becomes worse.

3.2 | Pediatric brain tumors: clinical applicability

Of 61 APTw scans performed in pediatric neuro-oncology patients at our center, we included 23 APTw scans of pediatric brain tumor patients in the final analysis (Figure 2). Data of one patient did not pass the quality control due to movement artifacts on APTw maps. Therefore, APTw

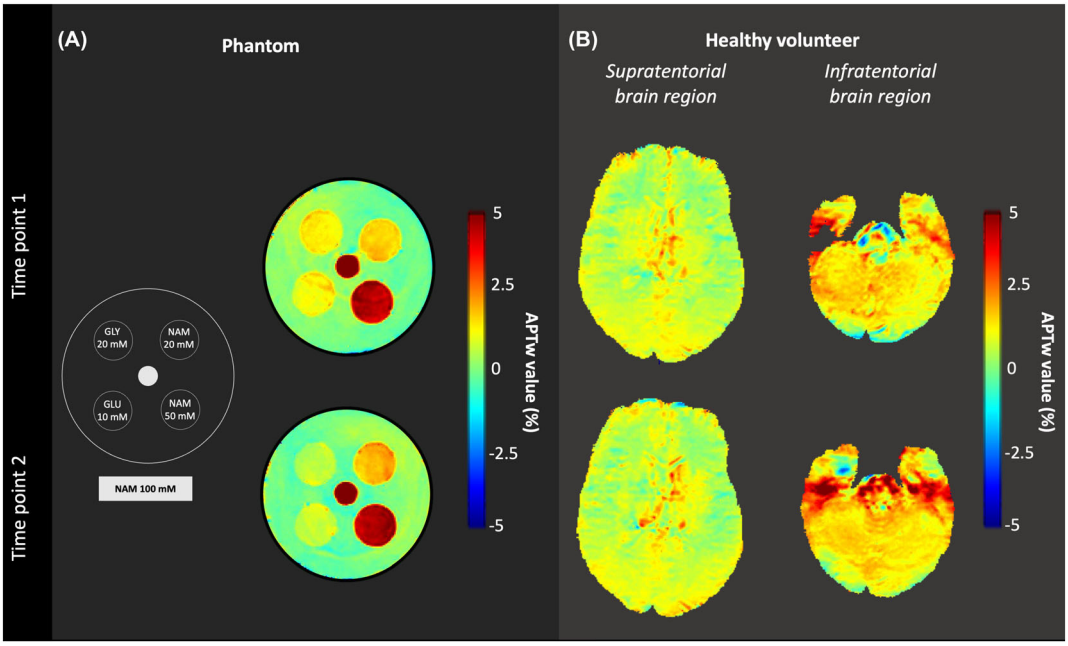

FIGURE 1 APTw maps of the phantom (A) and a healthy volunteer (supratentorial brain region and infratentorial brain region) (B) for two time points. Note the gap in the APTw map of the infratentorial brain region (Time Point 1) because there is no brain at this location (brain masking). GLU, glutamate; GLY, glycine; NAM, nicotinamide.

TABLE 1 Repeatability metric (wCV [%]) for phantom and healthy volunteers.

			APTw value (%) (mean ± STD)		
		Segment	Time Point 1	Time Point 2	wCV (%)
Phantom		ROI phantom			12
Healthy volunteers	Supratentorial brain region	GMs-ROI	0.74 ± 0.14	0.83 ± 0.08	13
		WMs-ROI	0.64 ± 0.19	0.75 ± 0.13	18
		eWMs-ROI	0.38 ± 0.36	0.51 ± 0.31	39
	Infratentorial brain region	GMc-ROI	1.71 ± 0.18	1.70 ± 0.18	11
		WMc-ROI	1.62 ± 0.24	1.66 ± 0.20	11
		eWMc-ROI	1.68 ± 0.42	1.80 ± 0.24	21
		WMp-ROI	1.45 ± 0.79	1.95 ± 0.75	50
		eWMp-ROI	1.56 ± 1.09	2.06 ± 0.78	39

Abbreviations: eWMc-ROI, eroded WM ROI of the cerebellum; eWMp-ROI, eroded WM ROI of the pons; eWMs-ROI, eroded WM ROI of the supratentorial brain region; GMc-ROI, gray matter ROI of the cerebellum; GMs-ROI, gray matter ROI of the supratentorial brain region; WMp-ROI, WM ROI of the pons; WMs-ROI, WM ROI of the supratentorial brain region.

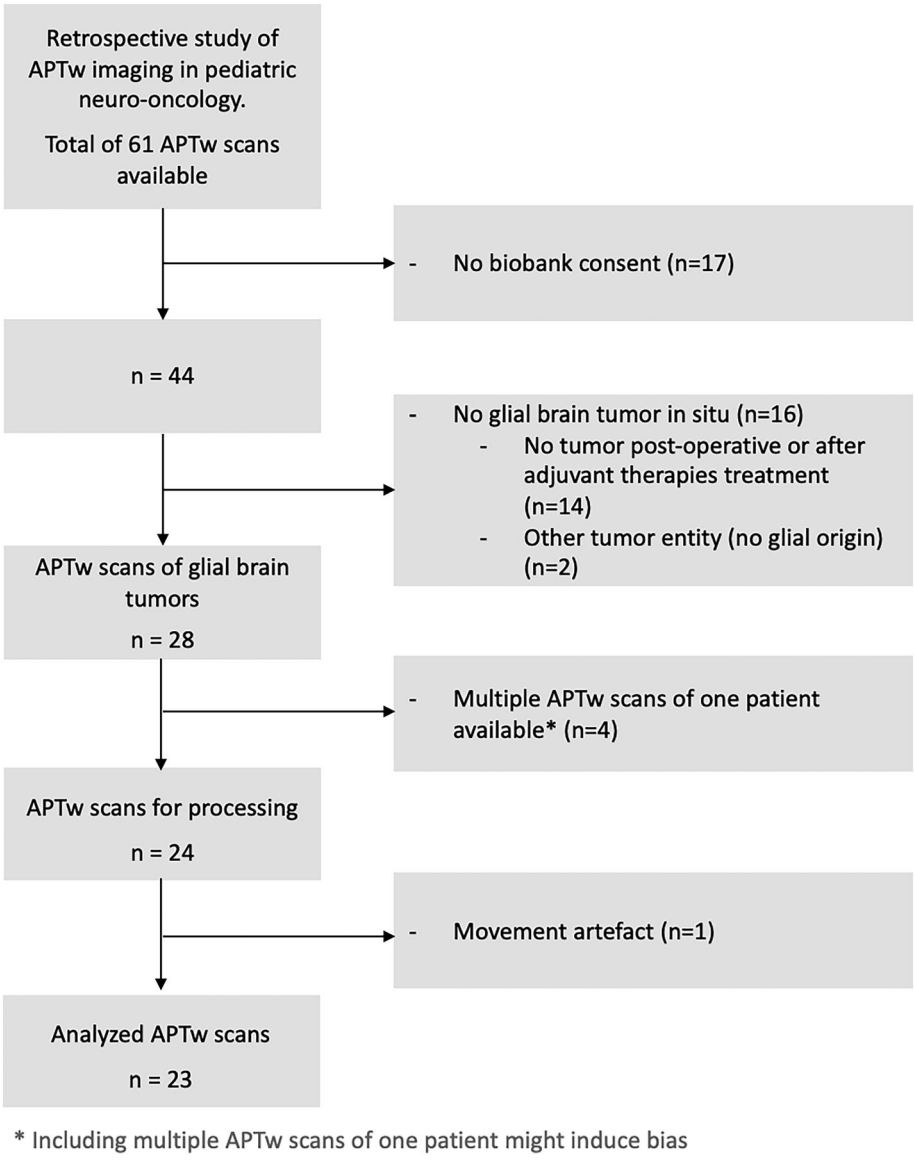

FIGURE 2 Study flowchart.

imaging of 23 children was used for analysis; baseline characteristics are shown in Table 2. An extensive overview of patient characteristics and corresponding APTw values of tumor and NAWM are given in Data S3.

Three examples of APTw imaging in pediatric brain tumors are shown in Figure 3. APTw values are significantly higher in tumors compared with NAWM for both pHGG and pLGG ($p = 0.001$ and $p < 0.001$, respectively) (Figure 4A). The mean APTw value was 2.58 ± 0.62 (range 1.80–

TABLE 2 Baseline characteristics of the 23 included patients.

	Total
Number	23
Sex, female (%)	11 (48)
Age, years (range)	12 ± 5 (2–17)
Time between diagnosis and MRI, months (range)	40 ± 51 (0–192)
MRI under anesthesia	6
Tumor volume (cc) (range)	23.99 ± 6.65 (0.47–90.71)
Tumor types	
pHGG[a]	7
pLGG[a]	16
Pilocytic astrocytoma	7
Other	4
No pathology available	5
Scan at diagnosis	5
Post-surgery	2
Scan during treatment	8
Wait-and-scan policy	8

[a]For detailed pathological diagnosis, see Data S3.

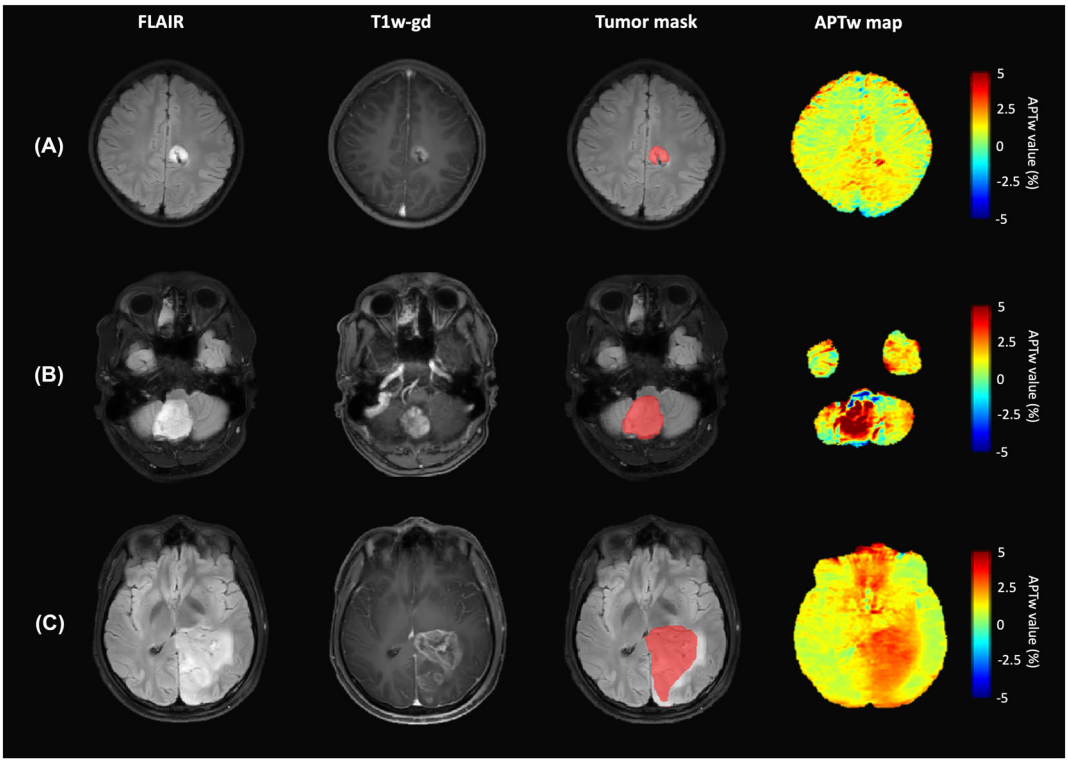

FIGURE 3 Three examples of APTw imaging, correlated anatomical scans, and tumor mask of different pediatric brain tumors: diffuse LGG (A), pilocytic astrocytoma (B), and pHGG (diffuse hemispheric glioma) (C).

3.50)% in pHGG (compared with 0.83 ± 0.52% in NAWM) and 2.32 ± 0.99 (range 1.10–4.66)% in pLGG (compared with 0.96 ± 0.35% in NAWM). The mean APTw value of pHGG was not higher than the mean APTw value of pLGG ($p = 0.46$). In patients with APTw imaging at diagnosis, patients with pLGG had low Ki-67 index and high APTw values, in contrast to patients with pHGG, who showed both a high Ki-67 index and high APTw values (see Data S3).

APTw values are significantly higher in pLGG subtype pilocytic astrocytoma compared with other pLGG subtypes (Figure 4B; $p = 0.047$). No statistically significant difference is present between mean APTw value of pilocytic astrocytoma and pHGG ($p = 0.30$), or between pHGG and other pLGG subtypes ($p = 0.07$).

Incorporation of fluid suppression in MTR_{asym} did not affect the APTw values in the solid tumor tissue (i.e., $n = 4$ APTw values were exactly identical; $n = 12$ APTw values were numerically, but not statistical significantly, lower, range 0.01%–0.58%). MTR_{asym} with fluid suppression seems to solely suppress fluid in cysts (Figure 5).

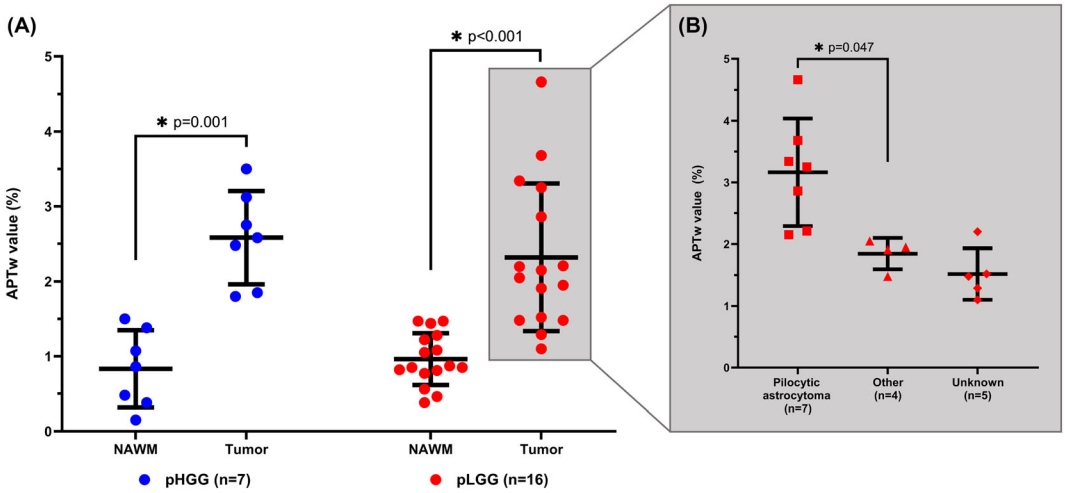

FIGURE 4 Plots of mean APTw values in pediatric brain tumor patients. APTw values of tumor and NAWM for pHGG and pLGG are shown. Gray panel: APTw values of subtypes of pLGG. * indicates significant difference.

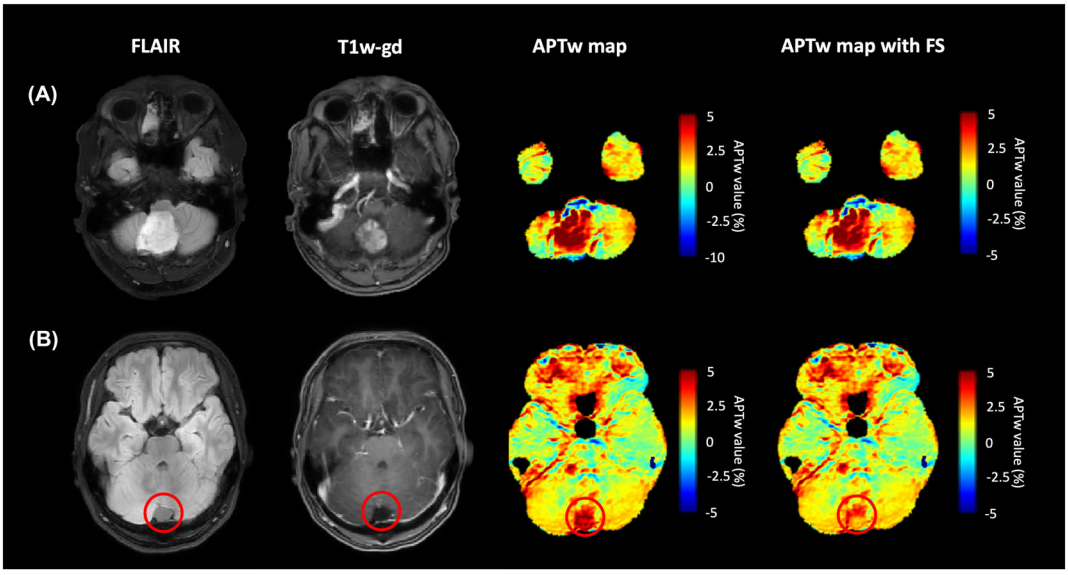

FIGURE 5 Example of 17-year-old male with a pilocytic astrocytoma encompassing a solid tumor part (A) and a cystic compartment (red circle) (B). APTw maps without and with fluid suppression (FS) are shown.

4 | DISCUSSION

We have shown that APTw values of pediatric glial brain tumors are higher than APTw values in NAWM of the same children. APTw values in pediatric brain tumors are, on average, 1.5 units higher compared with NAWM, which is larger than the wCV for supratentorial and infratentorial (cerebellar) ROIs. Therefore, APTw imaging allows for longitudinal assessment of tumors. A remarkable observation was that pilocytic astrocytomas have the highest mean APTw value, opening the possibility of radiologically differentiating pilocytic astrocytoma from other types of pLGG based on APTw imaging.

APTw imaging gives insight into tumor biology by providing information about endogenous protein and peptide concentrations in tissues.[9] Togao et al. showed that APTw values of adult brain tumors are correlated to the Ki-67 histopathological cell proliferation biomarker, indicating tumor aggressiveness.[24] As in adults, APTw values of pediatric brain tumors are significantly higher than APTw values of NAWM.[13] Overall, APTw values are in the same range as APTw values of pediatric and adult glioma mentioned in literature independent of tumor type.[25,26] However, unlike the study of Zhang et al.[25] in pediatric brain tumors, and studies in adult brain tumors,[27] we found no significant difference in APTw values between pHGG and pLGG. Unfortunately, we did not obtain APTw imaging at the same moment as the histopathological cell proliferation biomarker Ki-67 index. Therefore, we cannot exclude any correlation between APTw values and Ki-67 index based on this cohort of pediatric gliomas. The diagnostic performance of APTw imaging in differentiating pLGG and pHGG seems limited. However, this needs further investigation, given that a large number of patients in the pLGG group have a pilocytic astrocytoma, with high APTw values. Pilocytic astrocytoma is the most common subtype of pLGG, but is rare in adults.[28]

Histopathologically, pilocytic astrocytomas are defined as benign tumors with a low Ki-67 index. In this tumor, microvascular proliferation, microcysts, and mucoid material are frequently present.[29] Histological characteristics of pilocytic astrocytoma, especially microvascular proliferation, possibly explain the high APTw values. This might be similar to adult hemangioblastoma.[30] Furthermore, in essentially all pilocytic astrocytomas, MAPK pathway alterations are found to be the tumor driver, most often KIAA1549-BRAF (35%), BRAF V600E (17%), or NF1 (17%).[31] This pathway promotes cell growth and survival and reduces apoptosis.[32] In this study, all patients with a pilocytic astrocytoma had MAPK pathway alterations. However, all other pLGGs and some pHGGs also had MAPK pathway alterations as tumor driver, of which many cases displayed a rarer molecular alteration than most common tumor drivers mentioned above.

Many tumor characteristics, such as cysts, necrotic tumor areas, microvascular proliferation, and pH, seem to affect APTw values.[10] For example, exchange rates of protons are reduced in acid environments, such as ischemic stroke, which results in lower APTw values.[33] Higher APTw values in tumors can be explained by two elements: (1) higher concentrations of cytosolic proteins and peptides caused by increased cell density, and (2) a slightly higher intracellular pH increasing the exchange rates of the protons.[34] Furthermore, elevated levels of mobile proteins are not specific for solid tumor tissue since tumor cysts can contain high protein concentration as well. When interested in solid tumor tissue solely, signal of cystic fluids can be weighted such that their appearance in images is suppressed. Without this image post-processing step, APTw signal in cysts is high but not reflective of solid tumor tissue, which complicates discrimination between tumor components. Therefore, (patho)physiological processes should be considered for accurate interpretation of APTw maps by the radiologist.[11] Moreover, APTw values in normal brain tissue decline with age,[35,36] making age an important covariate to account for, particularly in the pediatric population.

The main limitation of this study is the small number of patients in each group. Also, the time between pathological diagnosis and APTw scan is relatively long in some patients. Pathological characteristics seem to be important to explain and interpret APTw values accurately. For validation of APTw imaging in pediatric neuro-oncology, pathology around scan time must be matched with APTw values (although pLGG rarely transforms towards high-grade malignancies[28]). Moreover, histological differences are present between pilocytic astrocytoma in the posterior fossa and optic pathways, showing a circumscriptive and more diffuse growth pattern, respectively.[29] APTw values are possibly affected by tumor location, and additionally areas with large B_0 inhomogeneities increase the complexity of accurate interpretation. Current implementation showed that APTw values are not reliable in the pontine area. Adjustment of acquisition parameters such as thinner slices and longer saturation pulse are expected to improve the reliability in this area. Finally, our APTw CEST acquisition is slightly different than recommended in a recent consensus paper,[34] in the sense that we measured with a larger offset interval (i.e., ±2.7, ±3.5, ±4.2 ppm instead of ±3.0, ±3.5, ±4.0 ppm), which may have resulted in a larger data interpolation error.

This study included a heterogeneous group of patients in comparison with literature.[25] Patients might not compromise a representative group of pediatric brain tumors, since APTw imaging was added to the protocol upon request of the radiologist with the consequence of potential selection bias. Furthermore, some patients ($n = 8$) underwent treatment prior to the acquisition of APTw images, while in other patients APTw imaging was performed at diagnosis or during a wait-and-scan policy. We cannot exclude eventual effects of treatment on APTw values in our study. For example, effect of bevacizumab, a monoclonal antibody against the vascular endothelial growth factor,[37] can be expected in pilocytic astrocytoma since this type of tumor has enhanced microvascular proliferation. Increased blood volume because of enhanced microvascular proliferation and/or mobile proteins leaking from this vasculature may result in high APTw values.[30] APTw values might reduce after bevacizumab treatment since it reduces microvascular proliferation. Treatment effects should be assessed in a longitudinal matter, which is possible since APTw maps are repeatable in cerebral and cerebellar brain regions. Further analysis should include comparable groups of pediatric brain tumors with and without treatment to investigate if longitudinal treatment-related changes in APTw values can be measured. This necessitates correlation of APTw maps

with clinical outcome parameters. Specific guidelines and/or cut-off values for clinical application regarding treatment effects of pediatric brain tumors can then be defined accordingly.

5 | CONCLUSION

Our study provides new insights into the radiological appearance of pediatric brain tumors on APTw maps. APTw values in glial tumors are significantly higher than those in NAWM in children, and high APTw values are present in pilocytic astrocytoma. Next steps should focus on the potential of APTw imaging in clinical decision-making aiming for longitudinal assessment of metabolic changes in pediatric brain tumors in response to therapy.

ACKNOWLEDGMENTS

We are indebted to Kim van de Ven (Philips Healthcare) for providing the APT sequence and for assisting with the implementation of the sequence. We would like to report financial support from the Wilhelmina Kinderziekenhuis (WKZ) research fund (Wijnen, 2018) and the Dutch Research Council (NWO) (Vidi-Wijnen-18361, Veni-Wiegers-18144). Funding sources had no role in this study.

CONFLICT OF INTEREST STATEMENT

The authors of this manuscript declare no relationships with any companies whose products or services may be related to the subject matter of the article.

ORCID

Iris V. Obdeijn https://orcid.org/0009-0001-3797-711X

REFERENCES

1. Richterová R, Kolarovszki B. Primary brain tumors in childhood. In: *Brain Tumors—an Update*. InTech; 2018. doi:10.5772/intechopen.74510
2. Keene DL, Johnston DL. Epidemiology of central nervous system tumors. In: *Pediatric Neuro-Oncology*. Springer; 2015:9-12. doi:10.1007/978-1-4939-1541-5_3
3. Udaka YT, Packer RJ. Pediatric brain tumors. *Neurol Clin*. 2018;36(3):533-556. doi:10.1016/j.ncl.2018.04.009
4. de Blank P, Bandopadhayay P, Haas-Kogan D, Fouladi M, Fangusaro J. Management of pediatric low-grade glioma. *Curr Opin Pediatr*. 2019;31(1):21-27. doi:10.1097/MOP.0000000000000717
5. Rashed WM, Maher E, Adel M, Saber O, Zaghloul MS. Pediatric diffuse intrinsic pontine glioma: where do we stand? *Cancer Metastasis Rev*. 2019;38(4):759-770. doi:10.1007/s10555-019-09824-2
6. Chukwueke UN, Wen PY. Use of the Response Assessment in Neuro-Oncology (RANO) criteria in clinical trials and clinical practice. *CNS Oncol*. 2019;8(1):CNS28. doi:10.2217/cns-2018-0007
7. Wen PY, Chang SM, van den Bent MJ, Vogelbaum MA, Macdonald DR, Lee EQ. Response assessment in neuro-oncology clinical trials. *J Clin Oncol*. 2017;35(21):2439-2449. doi:10.1200/JCO.2017.72.7511
8. Leao D, Craig P, Godoy L, Leite C, Policeni B. Response assessment in neuro-oncology criteria for gliomas: practical approach using conventional and advanced techniques. *Am J Neuroradiol*. 2020;41(1):10-20. doi:10.3174/AJNR.A6358
9. Wu B, Warnock G, Zaiss M, et al. An overview of CEST MRI for non-MR physicists. *EJNMMI Phys*. 2016;3(1):19. doi:10.1186/s40658-016-0155-2
10. van Zijl PCM, Yadav NN. Chemical exchange saturation transfer (CEST): what is in a name and what isn't? *Magn Reson Med*. 2011;65(4):927-948. doi:10.1002/mrm.22761
11. Zhou J, Heo HY, Knutsson L, van Zijl PCM, Jiang S. APT-weighted MRI: techniques, current neuro applications, and challenging issues. *J Magn Reson Imaging*. 2019;50(2):347-364. doi:10.1002/JMRI.26645
12. Su C, Liu C, Zhao L, et al. Amide proton transfer imaging allows detection of glioma grades and tumor proliferation: comparison with Ki-67 expression and proton MR spectroscopy imaging. *Am J Neuroradiol*. 2017;38(9):1702-1709. doi:10.3174/ajnr.A5301
13. Zhou J, Zhu H, Lim M, et al. Three-dimensional amide proton transfer MR imaging of gliomas: initial experience and comparison with gadolinium enhancement. *J Magn Reson Imaging*. 2013;38(5):1119-1128. doi:10.1002/jmri.24067
14. Ma B, Blakeley JO, Hong X, et al. Applying amide proton transfer-weighted MRI to distinguish pseudoprogression from true progression in malignant gliomas. *J Magn Reson Imaging*. 2016;44(2):456-462. doi:10.1002/jmri.25159
15. Jiang S, Eberhart C, Lim M, et al. Identifying recurrent malignant glioma after treatment using amide proton transfer-weighted MR imaging: a validation study with image-guided stereotactic biopsy. *Clin Cancer Res*. 2019;25(2):552-561. doi:10.1158/1078-0432.CCR-18-1233
16. Park JE, Kim HS, Park KJ, Kim SJ, Kim JH, Smith SA. Pre-and posttreatment glioma: comparison of amide proton transfer imaging with MR spectroscopy for biomarkers of tumor proliferation. *Radiology*. 2016;278(2):514-523. doi:10.1148/radiol.2015142979
17. Merchant TE, Pollack IF, Loeffler JS. Brain tumors across the age spectrum: biology, therapy, and late effects. *Semin Radiat Oncol*. 2010;20(1):58-66. doi:10.1016/j.semradonc.2009.09.005
18. D'Arco F, Culleton S, de Cocker LJL, Mankad K, Davila J, Tamrazi B. Current concepts in radiologic assessment of pediatric brain tumors during treatment, part 1. *Pediatr Radiol*. 2018;48(13):1-11. doi:10.1007/s00247-018-4194-9
19. van de Ven K, Keupp J. *Amide Proton Transfer Weighted Imaging: Advancement in Molecular Tumor Diagnosis*. White paper. Philips; 2018.

20. Togao O, Keupp J, Hiwatashi A, et al. Amide proton transfer imaging of brain tumors using a self-corrected 3D fast spin-echo Dixon method: comparison with separate B0 correction. *Magn Reson Med*. 2017;77(6):2272-2279. doi:10.1002/MRM.26322
21. Keupp J, Togao O. Magnetization transfer ratio based metric for APTw or CESTw MRI suppressing signal from fluid compartments—initial application to glioblastoma assessment. *Proc Int Soc Magn Reson Med*. 2018;26:3156.
22. Klein S, Staring M, Murphy K, Viergever M, Pluim J. Elastix: a toolbox for intensity-based medical image registration. *IEEE Trans Med Imaging*. 2010;29(1):196-205. doi:10.1109/TMI.2009.2035616
23. Yushkevich P, Piven J, Hazlett H, et al. User-guided 3D active contour segmentation of anatomical structures: significantly improved efficiency and reliability. *NeuroImage*. 2006;31(3):1116-1128. doi:10.1016/J.NEUROIMAGE.2006.01.015
24. Togao O, Yoshiura T, Keupp J, et al. Amide proton transfer imaging of adult diffuse gliomas: correlation with histopathological grades. *Neuro-Oncology*. 2014;16(3):441-448. doi:10.1093/neuonc/not158
25. Zhang H, Yong X, Ma X, et al. Differentiation of low- and high-grade pediatric gliomas with amide proton transfer imaging: added value beyond quantitative relaxation times. *Eur Radiol*. 31(12):9110-9119. doi:10.1007/s00330-021-08039-w/Published
26. Zhang H, Zhou J, Peng Y. Amide proton transfer-weighted MR imaging of pediatric central nervous system diseases. *Magn Reson Imaging Clin N Am*. 2021;29(4):631-641. doi:10.1016/J.MRIC.2021.06.012
27. Suh CH, Park JE, Jung SC, Choi CG, Kim SJ, Kim HS. Amide proton transfer-weighted MRI in distinguishing high- and low-grade gliomas: a systematic review and meta-analysis. *Neuroradiology*. 2019;61(5):525-534. doi:10.1007/s00234-018-02152-2
28. Sievert AJ, Fisher MJ. Pediatric low-grade gliomas. *J Child Neurol*. 2009;24(11):1397-1408. doi:10.1177/0883073809342005
29. Perry A, Wesseling P. Histologic classification of gliomas. *Handb Clin Neurol*. 2016;134:71-95. doi:10.1016/B978-0-12-802997-8.00005-0
30. Kamimura K, Nakajo M, Gohara M, et al. Differentiation of hemangioblastoma from brain metastasis using MR amide proton transfer imaging. *J Neuroimaging*. 2022;32(5):920-929. doi:10.1111/jon.13019
31. Ryall S, Zapotocky M, Fukuoka K, et al. Integrated molecular and clinical analysis of 1,000 pediatric low-grade gliomas. *Cancer Cell*. 2020;37(4):569-583. doi:10.1016/J.CCELL.2020.03.011
32. Srinivasa K, Cross KA, Dahiya S. BRAF alteration in central and peripheral nervous system tumors. *Front Oncol*. 2020;10:574974. doi:10.3389/FONC.2020.574974
33. Harston GWJ, Tee YK, Blockley N, et al. Identifying the ischaemic penumbra using pH-weighted magnetic resonance imaging. *Brain*. 2015;138(1):36-42. doi:10.1093/BRAIN/AWU374
34. Zhou J, Zaiss M, Knutsson L, et al. Review and consensus recommendations on clinical APT-weighted imaging approaches at 3T: application to brain tumors. *Magn Reson Med*. 2022;88(2):546-574. doi:10.1002/MRM.29241
35. Zhang H, Kang H, Zhao X, et al. Amide proton transfer (APT) MR imaging and magnetization transfer (MT) MR imaging of pediatric brain development. *Eur Radiol*. 2016;26(10):3368-3376. doi:10.1007/S00330-015-4188-Z/METRICS
36. Mennecke A, Khakzar KM, German A, et al. 7 tricks for 7 T CEST: improving the reproducibility of multipool evaluation provides insights into the effects of age and the early stages of Parkinson's disease. *NMR Biomed*. 2023;36(6):e4717. doi:10.1002/NBM.4717
37. Zhukova N, Rajagopal R, Lam A, et al. Use of bevacizumab as a single agent or in adjunct with traditional chemotherapy regimens in children with unresectable or progressive low-grade glioma. *Cancer Med*. 2018;8(1):40-50. doi:10.1002/cam4.1799

SUPPORTING INFORMATION

Additional supporting information can be found online in the Supporting Information section at the end of this article.

How to cite this article: Obdeijn IV, Wiegers EC, Alic L, et al. Amide proton transfer weighted imaging in pediatric neuro-oncology: initial experience. *NMR in Biomedicine*. 2024;37(6):e5122. doi:10.1002/nbm.5122